RJC

RASĀYAN *J. Chem.*
Vol. 18 | No. 3 |1495-1502| July-September | 2025
ISSN: 0974-1496 | e-ISSN: 0976-0083 | CODEN: RJCABP
http://www.rasayanjournal.com
http://www.rasayanjournal.co.in

THERMAL EFFECTS AND ADSORPTION BEHAVIOR OF A FEW GREEN AND SYNTHETIC INHIBITORS ON API5LX60 STEEL IN CO_2-SATURATED SALINE MEDIA

P. Burhagohain[1], G. Sharma[2,✉], S. Sarmah[1] and S. Priyadarshini[1]
[1]Department of Chemistry, Dibrugarh University, Dibrugarh-786004, Assam, India
[2]Department of Chemistry, DUIET, Dibrugarh University, Dibrugarh-786004, Assam, India
✉Corresponding author: gitaleesharma@dibru.ac.in

ABSTRACT

The transportation of crude oil and natural gas employs steel pipes as an economic engineering material. However, despite its mechanical strength, it undergoes corrosion under drastic environmental conditions. In this line, temperature plays a pivotal role in the electrochemical processes of steel, whenever it encounters a corrosive medium, which is very often devastating. This paper, thus, reports the temperature effect at 298K, 303K, 313K, 323K and 333K on corrosion rates of three oxazolone derivatives, three plant extracts and blends of oxazolone derivatives with two plant extracts coated API5LX60 steel in 3.5% NaCl solution with CO_2 saturation using gravimetric analysis data. The results revealed that increased temperature elevated the corrosion rate and depleted the % inhibition efficiency considerably. This outcome is consistent for all corrosion inhibitors examined, regardless of the inhibitor concentration. Three different adsorption isotherms obeyed by the reported inhibitors have also been considered with data from gravimetric analysis. The mode of adsorption was affirmed as physisorption, with the best fit given by the Langmuir adsorption isotherm, with the linear regression coefficient (R^2) value approx. to one. This work thus has a significant contribution to both academic researchers and industrial corrosion engineers as it will serve as a valuable reference against thermal and adsorption modelling in the CO_2 environment of synergistic synthetic and green corrosion inhibitors.

Keywords: Corrosion Inhibitor, API5LX60 Steel, Thermodynamics, Adsorption, CO_2 Environment.
RASĀYAN *J. Chem.*, Vol. 18, No.3, 2025

INTRODUCTION

The worldwide prime concern for pipeline corrosion is alarming, as it costs the global economy over $2.5 trillion annually.[1] The petroleum industries rely heavily on steel as a cost-effective engineering material for the recovery and transportation of crude oil and natural gas. However, the efficacy of steel is often restricted by aggressive corrosion due to acidic transportation of crude oil and natural gas, and moisture-rich environmental aspects.[2] In this context, CO_2, which can cause localized corrosion of mild steel, has played a key role as it can lead to destruction without other complicating factors. To mitigate this issue, organic corrosion inhibitors are known to be used widely by all such industries. Organic compounds containing atoms, viz nitrogen, oxygen, sulphur, phosphorus, and π-conjugated groups, render them viable candidates for anti-corrosive inhibitors.[3] These compounds have the momentous property of adsorbing onto the metal surface, effectively interfering with the electrochemical process of corrosion by either physisorption or chemisorption. In this vein, thermodynamics and adsorption behavior are vivacious aspects in understanding the mechanism of functioning of these inhibitors.[4] Further, temperature plays a significant role in the electrochemical process that occurs during corrosion of a metal whenever it encounters a corrosive medium.[5] The consequences of temperature change on inhibited corrosive medium are quite involved, as the metal surface may undergo various changes like disruption, desorption, or decomposition of the applied inhibitor. Konovalova, in his research, revealed that metals in a corrosive environment undergo dissolution faster on the surface of high carbon content alloys.[6] Again, Li *et.al.* investigated the temperature dependence of Copper–Aluminum Laminated Composite Plate on corrosion and observed that the corrosion resistance of these plates decreased considerably with an increase in temperature, and the worst effect was at 50 ºC.[7] Further, Moro *et al.* went off track and predicted the temperature dependence of corrosion rate on service life estimation.[8] Furthermore, Quan and his co-workers evaluated the temperature

http://doi.org/10.31788/RJC.2025.1839246

effect on the corrosion of Q235 steel and 16Mn steel in the sodium aluminate solution, and the results showed that the corrosion rates of the two steels increased with temperature, which was further more for the Q235 steel compared to that of 16Mn steel at higher temperatures.[9] Even though steel pipelines are crucial to comprehensive energy transport, their corrosion at high temperatures in CO_2 environments remains insufficiently understood. Thus, there is a need to study the effect of temperature at a certain concentration of inhibitor on corrosion rate and inhibition efficiencies.[10] In this paper, the effect of temperature on the rate of corrosion and related thermodynamic parameters has been reported. The temperature effect at 298K, 303K, 313K, 323K, and 333K on corrosion rates of oxazolone derivatives, three plant extracts, and blends of oxazolone derivatives with two plant extracts coated API5LX60 steel in 3.5% NaCl solution with CO_2 saturation was studied using gravimetric analysis data. The evaluation of different adsorption isotherms obeyed by the studied inhibitor has also been considered based on the data obtained from gravimetric analysis. Adsorption studies also highlight a mechanism for the inhibitory action of the studied inhibitor. Further, this work aligns with the United Nations Sustainable Development Goals (SDGs) 12: Responsible Consumption and Production by promoting the use of green and hybrid corrosion inhibitors, contributing to robust environment-friendly designs, and by encouraging sustainable chemical usage, which will reduce the ecological footprint of pipeline maintenance and materials use. This supports and reduces environmental pollution from industrial additives.

EXPERIMENTAL

Materials and Methods

All the chemicals used were commercially obtained. The API5LX60 steel samples were procured from the pipelines in the oilfields of Oil India Limited, Duliajan, Assam. Ethanol and acetone were obtained from Merck. Sodium Chloride (NaCl) salt was procured from Fischer Scientific. All solvents were distilled before use.

Preparation of Steel Sample for Gravimetric Studies

For the Gravimetric weight loss analysis, API5LX60 steel pipe samples were cut into coupons of dimension 3.5cm x 0.7cm x 0.6 cm and exposed surface area 2.45cm^2. The steel coupons were polished with different grades of emery papers, washed with double-distilled water, degreased with acetone, and then dried at 60-70 ^{0}C before the start of the experiment. Fig.-1(a and b) depict steel samples with and without inhibitor coating.

(a) (b)

Fig.-1: Steel Sample (a) Uninhibited (b) Inhibitor Coated

Test solutions were prepared by dissolving 3.5 g anhydrous NaCl in 100 mL of double-distilled water, saturated with CO_2 at a gas pressure of 700 kPa. A high-pressure gas Adsorption System was used for CO_2 adsorption. The gravimetric weight loss data for three oxazolone derivatives 2-Methyl-4-naphthalen-2-ylmethylene-4H-oxazol-5-one (ON), 4-(2-Methyl-5-oxo-oxazol-4-ylidenemethyl)-benzaldehyde (OT), and 4-(2-Methyl-5-oxo-oxazol-4-ylidenemethyl)-benzene (OB), three plant extracts viz. *Eclipta alba* (EA), *Moringa oleifera* (MO), and *Murraya koenigii* (MK), and the blends of ON, OT, OB with EA and MO were the samples under examination.[11-13] The gravimetric weight loss analysis was carried out for the synthesized inhibitor to study the effect of temperature at 298K, 303K, 313K, 323K, and 333K on corrosion rate and inhibition efficiency. The weight loss data at 298K were taken from previous studies for oxazolone[11], plant extracts, and their blends, respectively.[11-13] The samples were immersed in the test solution in both uninhibited and inhibited conditions while maintaining a steady temperature of 298K, 303K, 313K, 323K, and 333K, respectively, for an immersion period of 1 hour each. The inhibitor concentration for the temperature study

was 50, 100, 150, and 200 ppm for oxazolone derivatives and 40, 60, 80, and 100 ppm for plant extracts and blends.

Thermodynamic and Adsorption Studies

Again, the investigation of corrosion parameters under different temperature conditions helps to determine the energy of activation for both corrosion and inhibition processes. Activation parameters are also important to understand the mechanism of inhibition of mild steel. In general, the rate of electrochemical processes increases with an increase in temperature, which in turn affects adsorption and kinetic parameters.[5,9] Corrosion being an electrochemical process, the rate of corrosion can be related to the energy of activation by the Arrhenius type equation as given in equation (1).[5]

$$CR = A \exp\left(-{E_a}/{RT}\right) \quad (1)$$

Where, E_a the energy of activation, A, is the Arrhenius pre-exponential factor, T is the absolute temperature, and R is the Universal Gas Constant. Taking the logarithm of equation (1) gives equation (2).[5]

$$\log CR = \log A - \frac{E_a}{2.303RT} \quad (2)$$

A plot of log CR versus 1/T will be a straight line with slope $-\frac{E_a}{R}$ and intercept log A. This plot thus allows for the calculation of the energy of activation for corrosion.[6,14]

Again, the steel surface interaction with corrosion inhibitors can be best understood by studying the adsorption isotherm. Most frequently used isotherms are Langmuir, Temkin, Freundlich, etc., having the general form as given in equation (3).[6,14]

$$f(\theta, x)\exp(-2a, \theta) = kc \quad (3)$$

Where, $f(\theta, x)$ is a configurational factor that depends on the physical model, θ is the surface coverage, k is the equilibrium constant, and c is the inhibitor concentration. x is the size ratio indicating the number of water molecules replaced by the inhibitor. θ can be evaluated using equation (4).[15]

$$\theta = \frac{\%IE}{100} \quad (4)$$

The equilibrium constant can be determined from the intercept of adsorption isotherm plots. Three different isotherms were studied to see which isotherm showed the best fit. However, all three adsorption isotherms, Langmuir, Tempkin, and the Freundlich adsorption isotherm, showed the same results.

Langmuir isotherm is a plot of C/θ versus C, as shown in equation (5).

$$\frac{C}{\theta} = \frac{1}{k_{ads}} + C \quad (5)$$

$\frac{C}{\theta}$ was plotted against C for different θ values at various temperatures, and a straight line should be obtained, having a linear regression coefficient (R^2) value close to unity, suggesting that the observed data fit well to the Langmuir isotherm.[16]

The Tempkin adsorption isotherm has the form given in equation (6).

$$\theta = \frac{2.303RT}{b}\log C + \frac{2.303RT}{b} log k_{ads} \quad (6)$$

Where b (kJ/mol) is a constant related to the heat of adsorption. Thus, a plot of θ versus log C gives the Temkin isotherm, whose intercept gives the value of k_{ads}. b can be evaluated from the slope of the Temkin isotherm.[17]

The Freundlich adsorption isotherm can be represented by equations (7 & 8) given below:

$$\theta = k_{ads}C^n \quad (7)$$

$$or, log\theta = \frac{1}{n} logC + log k_{ads} \quad (8)$$

A plot of log θ against log C represents the Freundlich isotherm, which should be a straight line.[18] The equilibrium constant can be determined from the intercept of the isotherm.

RESULTS AND DISCUSSION

The corrosion parameters obtained from gravimetric analysis at different temperatures of 298K, 303K, 313K, 323K, and 333K are tabulated in Table-1, Table-2, and Table-3 for oxazolone, plant extract, and their blends, respectively.

Table-1: Corrosion Parameter Obtained for Oxazolone Inhibitor at Different Temperatures[12]

Inhibitor name	IC (ppm)	298 K		303 K		313 K		323 K		333 K	
		CR (mmpy)	%IE	CR (mmpy)	%IE	CR (mmpy)	%IE	CR (mmpy)	%IE	CR (mmpy)	%IE
ON	0	13.36	0	13.71	0	14.06	0	14.44	0	15.11	0
	50	6.39	52.17	6.38	52.14	6.97	51.98	7.11	51.03	8.06	49.89
	100	5.23	60.86	5.30	60.23	5.11	60.01	5.87	59.79	6.37	56.44
	150	2.90	78.26	2.97	78.13	3.23	77.87	3.98	77.16	4.14	76.53
	200	1.16	91.30	1.36	91.02	1.98	90.76	2.41	90.44	2.99	89.59
OT	0	13.36	0	13.71	0	14.06	0	14.44	0	15.11	0
	50	7.56	43.47	8.13	43.09	8.78	42.20	9.36	41.77	9.98	41.03
	100	5.81	56.52	6.68	55.98	7.13	55.04	7.98	54.33	8.12	53.31
	150	5.23	60.86	5.97	60.03	6.14	58.45	6.59	58.06	6.87	57.64
	200	2.32	82.60	2.41	81.96	2.98	81.32	3.45	80.56	3.88	80.04
OB	0	13.36	0	13.71	0	14.06	0	14.44	0	15.11	0
	50	7.30	39.13	7.99	39.00	7.99	38.32	8.73	37.36	9.68	36.32
	100	6.39	52.17	6.87	51.87	6.87	51.13	7.90	50.56	8.12	49.44
	150	4.06	69.56	4.34	69.22	4.34	68.30	5.56	67.68	6.68	67.03
	200	2.90	78.26	3.03	78.03	3.03	77.95	3.98	77.11	4.57	76.45

Table-2: Corrosion Parameter Obtained for Plant Extract Inhibitor at Different Temperatures[13]

Inhibitor name	IC (ppm)	298 K		303 K		313 K		323 K		333 K	
		CR (mmpy)	%IE	CR (mmpy)	%IE	CR (mmpy)	%IE	CR (mmpy)	%IE	CR (mmpy)	%IE
EA	0	14.97	0	15.24	0	15.77	0	16.05	0	16.97	0
	40	8.36	43.75	8.67	42.11	9.01	40.97	9.49	40.05	9.91	38.97
	60	5.11	65.62	5.40	6.23	5.81	60.01	6.03	59.79	6.40	56.44
	80	3.25	78.12	3.54	78.13	3.73	77.87	4.12	77.16	4.54	76.53
	100	1.39	90.63	1.71	89.03	2.03	88.45	2.48	86.98	2.98	85.76
MO	0	14.97	0	15.24	0	15.77	0	14.44	0	16.97	0
	40	8.33	37.50	8.13	37.00	8.78	36.65	9.36	34.98	9.98	33.87
	60	6.04	59.37	6.68	58.86	7.13	58.04	7.98	56.78	8.12	55.98
	80	4.18	71.87	5.97	70.02	6.14	68.45	6.59	67.57	6.87	65.66
	100	1.86	87.5	2.41	86.67	2.98	85.44	3.45	84.36	3.88	82.34
MK	0	14.97	0	15.24	0	15.77	0	14.44	0	16.97	0
	40	10.69	28.12	10.98	27.00	11.25	26.65	11.76	25.01	12.02	24.69
	60	6.51	56.25	6.89	55.23	7.45	54.87	7.96	53.16	8.32	52.87
	80	4.65	68.75	4.91	67.04	5.29	66.54	5.71	65.52	6.88	65.03
	100	2.32	84.37	3.10	83.32	3.53	82.21	3.90	81.15	4.59	80.23

Table-3: Corrosion Parameter Obtained for the Blend Inhibitor at Different Temperatures

Inhibitor name	IC (ppm)	298 K		303 K		313 K		323 K		333 K	
		CR (mmpy)	%IE	CR (mmpy)	%IE	CR (mmpy)	%IE	CR (mmpy)	%IE	CR (mmpy)	%IE
OBEA	0	14.97	0	15.28	0	15.69	0	16.17	0	16.89	0
	40	7.32	51.25	7.87	50.76	8.11	50.06	8.98	49.43	9.43	48.04
	60	5.91	64.68	6.36	63.54	6.87	63.05	7.65	62.87	8.21	62.11
	80	3.22	74.05	3.56	73.65	4.03	73.04	4.57	72.45	5.03	71.56
	100	1.09	82.5	1.38	81.98	1.99	81.23	2.37	80.45	2.81	79.66
OBMO	0	14.97	0	15.28	0	15.69	0	16.17	0	16.89	0
	40	7.62	50.93	8.13	50.13	8.78	49.65	9.36	48.87	9.98	48.23
	60	5.99	61.25	6.68	60.88	7.13	60.03	7.98	59.44	8.12	58.33
	80	3.37	72.5	5.97	71.65	6.14	70.97	6.59	70.01	6.87	69.23
	100	1.10	81.56	2.41	81.05	2.98	80.43	3.45	80.09	3.88	79.34
OTEA	0	14.97	0	15.28	0	15.69	0	16.17	0	16.89	0
	40	6.03	57.5	7.99	57.04	7.99	56.65	8.73	56.04	9.68	55.32
	60	4.01	70.93	6.87	70.41	6.87	69.85	7.90	69.23	8.12	68.54
	80	2.20	82.46	2.54	82.11	2.99	81.65	3.65	81.03	4.03	80.5
	100	0.99	89.96	1.32	89.35	1.76	88.67	2.33	88.18	2.78	87.24
OTMO	0	14.97	0	15.28	0	15.69	0	16.17	0	16.89	0
	40	6.11	55.93	5.57	55.33	5.04	54.67	4.54	54.03	4.41	53.31

	60	4.23	69	4.57	68.45	5.04	67.90	5.55	67.23	5.89	66.37
	80	2.83	75.96	3.09	75.34	3.57	74.73	3.98	74.21	4.65	73.59
	100	0.99	85.93	1.13	85.34	1.45	84.89	1.95	84.32	2.36	83.88
ONEA	0	14.97	0	15.28	0	15.69	0	16.17	0	16.89	0
	40	5.11	64.68	5.34	64.23	5.97	63.72	6.44	63.05	6.90	62.50
	60	3.89	76.96	4.21	76.30	4.69	75.84	4.90	75.06	5.57	74.68
	80	2.00	89.65	2.34	89.21	2.78	88.78	3.09	88.24	3.65	87.80
	100	0.71	94.84	1.16	94.56	1.47	94.0	1.90	93.57	2.47	92.97
ONMO	0	14.97	0	15.28	0	15.69	0	16.17	0	16.89	0
	40	5.36	60	5.88	59.75	6.09	59.04	6.79	58.35	7.49	57.63
	60	3.99	68.8	4.22	68.21	4.67	67.76	4.95	67.11	5.37	66.65
	80	2.14	85.87	2.35	85.27	2.87	84.78	3.50	84.28	3.93	83.79
	100	0.89	92.43	1.06	92.05	1.44	91.67	1.79	91.05	2.15	90.69

From Table-(1, 2, and 3), it is apparent that with an increase in temperature corrosion rate increases and the inhibition efficiency decreases. For the uninhibited solution increase in corrosion rate is more pronounced than in the inhibited solutions. This variation in corrosion rate and % Inhibition efficiency is valid for all three sets of inhibitors, viz., oxazolone derivatives, plant extracts, and the blends of plant extracts with oxazolones discussed in this article. The impact of the temperature on the % Inhibition efficiency may be explained in the way that adsorption of the inhibitor on the metal surface is through physisorption or chemisorption. Coordinate bonds between the inhibitor molecules and the metal surface are expected to be formed via the donation of lone electron pairs of heteroatoms to the empty orbitals of iron atoms. This explanation aligns with all three types of inhibitors. Further, the calculation of the energy of activation of corrosion and inhibition processes was conducted with the corrosion parameters for the prototype ON inhibitor. Fig.-2 below shows a plot of log CR versus 1/T at different inhibitor concentrations of ON. The E_a values obtained from the slope of the plot at different inhibitor concentrations of the same are tabulated in Table-4.

Table-4: Thermodynamic Parameters Obtained from Graph Fitting for *ON*

Solution(in ppm)	R^2	E_a(kJ/mol)	ΔH^0(kJ/mol)	IncrementS^0(J/Kmol)
Blank	0.977	2.56	0.69	-174.07
50ppm	0.642	3.81	2.57	-174.19
100ppm	0.913	4.50	3.86	-177.58
150 ppm	0.947	9.07	7.02	-182.38
200ppm	0.991	22.08	19.52	-217.16

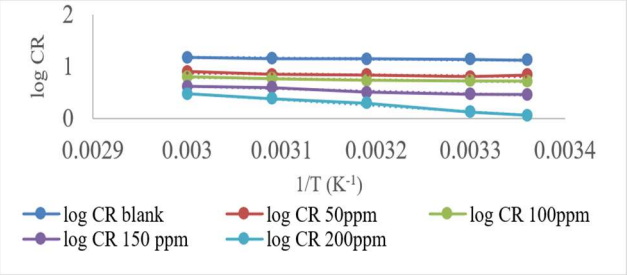

Fig.-2: Plot of log CR vs 1/T of ON Inhibitor

E_a for the inhibited solutions are much higher than the uninhibited solution, which further increases with an increase in inhibitor concentration. An increase in activation energy indicates a decrease in the rate of corrosion because of the adsorption of the inhibitor on the electrode-electrolyte interface, which acts as a shield for the transfer of charge and mass. Thus, it can also be concluded that the process of increasing inhibition and decreasing corrosion rate with an increase in inhibitor concentration is due to an increase in the energy of activation of the corrosion process. E_a value ranges from 2.56 to 22.08 kJ/mol. The threshold energy barrier for chemisorption to occur is 80kJ/mol, i.e., below 80 kJ/mol suggests a physisorption mechanism, and above 80kJ/mol a chemisorption process. Thus, the E_a value signifies that the adsorption of the studied inhibitor compound occurs via physisorption on the API5LX60 steel surface. Some other important thermodynamic parameters like enthalpy (ΔH^0) and entropy (ΔS^0), which will validate the

mechanism of corrosion, can be calculated using the reaction rate of the transition state equation given in equation (9).[5,6]

$$CR = \frac{RT}{Nh}\exp\left(-\frac{\Delta H^0}{RT}\right).\exp\left(\frac{\Delta S^0}{R}\right)$$

$$\text{Or,} \quad \frac{CR}{T} = \frac{R}{Nh}\exp\left(-\frac{\Delta H^0}{RT}\right).\exp\left(\frac{\Delta S^0}{R}\right) \qquad (9)$$

Where T is absolute temperature, R is the Universal Gas Constant, N is Avogadro's no, and h is Planck's constant. Taking the log of equation (9), equation (10) is obtained.[5]

$$\log\frac{CR}{T} = -\frac{\Delta H^0}{2.303RT} + \log\frac{R}{Nh} + \frac{\Delta S^0}{2.303R} \qquad (10)$$

When log (CR/T) is plotted against 1/T, a straight line is obtained having slope $-{}^{\Delta H^0}/_{2.303R}$ and intercept $\log {}^{R}/_{Nh} + {}^{\Delta S^0}/_{2.303R}$ as depicted in Fig.-3. Thus, from the slope and intercept, enthalpy and entropy can be determined.[17] The values ΔH^0 and ΔS^0 obtained from plotting log (CR/T) against 1/T for the ON inhibitor have been tabulated in Table-4. In general, the values of ΔH° lower than 43.2 kJ/mol are attributed the physical adsorption, and the values within the range 43.2 kJ/mol to 100kJ/mol indicate chemical adsorption.[19] From Table-4, it was found that the values of activation of enthalpy range from 2.57 KJ/mol to 19.52 KJ/mol in the presence of the ON inhibitor compound, indicating physisorption of the inhibitor compound on mild steel. A positive sign of activation of enthalpy reflects the endothermic nature of the carbon steel dissolution process.[20] The increase in enthalpy with inhibitor concentration affirms that kinetic parameters control the decline in corrosion rates. The negative values of ΔS° affirmed the association of the possible activated complex of the rate-determining step, thereby suggesting a decrease in randomness on going from reactants to the activated complex.[21-24] The adsorption behaviour of the three oxazolone derivatives, the three plant extracts, and blending extracts has been studied using Langmuir, Temkin, and Freundlich adsorption isotherms. Langmuir isotherms obtained at different temperatures are the reciprocal of the intercept, and they give the equilibrium constant of the adsorption process, k_{ads}. In the case of the Temkin adsorption isotherm, the experimental data fitted well to the isotherm with an R^2 value close to unity. Similarly, in the Freundlich isotherm, the equilibrium constant can be determined from the intercept of the isotherm. The values of k_{ads} and R^2 obtained at different temperatures, fitting to all three adsorption isotherms for the studied samples in CO_2 saturated 3.5% NaCl test solution are tabulated in Table-5. From the Table-5, it was observed that the change in Gibbs' free energy of adsorption was found to be between -20 to -40 kJ/mol suggesting strong physical adsorption of the studied inhibitor on the surface of API5LX60 steel. The R^2 values for all three isotherms were in consonance; however, it more aligned with the Langmuir adsorption isotherm, with values very close to unity for all the studied inhibitors. The adsorption studies were also in accordance with the thermodynamic studies.

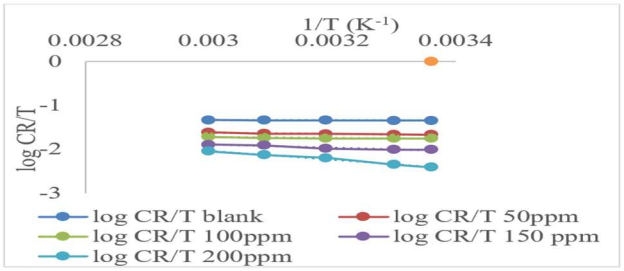

Fig.-3: Plot of log CR/T vs 1/T of ON Inhibitor

Thus, this study focuses on the fact that elevated temperature significantly accelerates corrosion in CO_2-saturated 3.5% NaCl environments, while simultaneously lowering the % inhibition efficiency of all the studied corrosion inhibitors. The corrosion inhibition performance showed a decline across all concentrations, emphasizing a critical limitation in current inhibitor technologies under thermal stress. Again, since the adsorption mechanism is physisorption, this study provides molecular-level insight into the interaction between inhibitors and the steel surface. This mechanistic understanding is vital in designing

thermally stable and environmentally benign corrosion inhibitors. Further, this work aligns with SDG 12 (Responsible Consumption and Production) as the results imply that by improving the understanding of temperature-dependent corrosion behavior and adsorption efficiency, it will enable better protection strategies, thereby extend the service life of steel materials, and promote resource efficiency.

Table-5: Adsorption and Thermodynamic Parameters Obtained for Different Inhibitor Systems

Inhibitor name	Adsorption isotherm								
	Langmuir			Temkin			Freundlich		
	k_{ads} (ppm)	R^2	ΔG^0_{ads}	k_{ads} (ppm)	R^2	ΔG^0_{ads}	k_{ads} (ppm)	R^2	ΔG^0_{ads}
ONEA	0.020	0.9688	-24.536	0.028	0.9719	-25.343	0.517	0.9688	-32.594
ONMO	0.018	0.9952	-24.247	0.016	0.9719	-24.029	0.584	0.9586	-32.896
OTEA	0.011	0.9267	-23.032	0.021	0.978	-24.680	0.372	0.9373	-31.778
OTMO	0.017	0.9751	-24.191	0.020	0.7121	-24.585	0.525	0.6904	-32.632
ON	0.026	0.9745	-25.167	0.046	0.8839	-26.600	0.553	0.8982	-32.761
OT	0.029	0.9917	-25.491	0.014	0.9798	-23.739	0.719	0.9594	-27.706
OB	0.026	0.9992	-25.224	0.014	0.9856	-23.599	0.772	0.9899	-27.882
EA	0.017	0.9948	-24.089	0.027	0.9772	-25.316	0.425	0.9504	-26.404
MO	0.015	0.988	-23.889	0.029	0.9851	-25.524	0.421	0.9425	-26.380
MK	0.061	0.999	-27.311	0.036	0.9181	-26.013	0.419	0.9082	-26.368

CONCLUSION

The influence of temperature at 298K, 303K, 313K, 323K, and 333K on the corrosion rates of oxazolone derivatives, three plant extracts, and blends of oxazolone derivatives with two plant extracts coated on API5LX60 steel in a 3.5% NaCl solution with CO_2 saturation was investigated using gravimetric analysis. The results showed a noteworthy elevation in the corrosion rate and decline in % inhibition efficiency with a rise in temperature, indicating thermal sensitivity of the inhibition mechanism. The adsorption behavior closely followed the Langmuir isotherm, suggesting monolayer coverage and physical adsorption. The outcome underlined the need for designing thermally stable and eco-friendly corrosion inhibitors to enhance pipeline durability. The work contributes not only to corrosion science but also supports sustainable industrial practices in line with SDG 12 by promoting the use of green, resource-efficient corrosion mitigation strategies.

ACKNOWLEDGMENTS

The authors acknowledge the DST PURSE project, Dibrugarh University (SR/PURSE/2022/143(C)) for funding the project.

CONFLICT OF INTERESTS

The authors declare that there is no conflict of interest.

AUTHOR CONTRIBUTIONS

The present work is related to *SDG-12: Responsible Consumption and Production*. All the authors contributed significantly to this manuscript, participated in reviewing/editing, and approved the final draft for publication. The research profile of the authors can be verified from their ORCID ids, given below:

P. Burhagohain https://orcid.org/0000-0003-2998-4368
G. Sharma https://orcid.org/0000-0002-3957-6862
S. Sarmah http://orchid.org/0009-0003-2444-8694
S. Priyadarshini https://orcid.org/0009-0007-0883-6821

REFERENCES

1. E. Shekari, F. Khan and S. Ahmed, *International Journal of Pressure Vessels and Piping*, **137**, 13(2016), https://doi.org/10.1016/j.ijpvp.2015.04.014

2. A. Nahlé, M. Al-Khayat, I. I. Abu-Abdoun and I. Abdel-Rahman, *Anti-Corrosion Methods and Materials*, **60(1)**, 20(2013), https://doi.org/10.1108/00035591311287410
3. J. Li, C. Sun, M. Roostaei, M. Mahmoudi, V. Fattahpour, H. Zeng, and J. Luo, *Society of Petroleum Engineers Thermal Integrity and Design Symposium*, D011S003R004(2019), https://doi.org/10.2118/198703-MS
4. A. F. S. A. Rahiman and S. Sethumanickam, *Arabian Journal of Chemistry*, **10(2)**, S3358(2017), https://doi.org/10.1016/j.arabjc.2014.01.016
5. S. Manimegalai and P. Manjula, *Journal of Materials and Environmental Science,* **6 (6)**, 1629(2015).
6. V. Konovalova, *Materials Today: Proceedings*, **38(4)**, 1326(2021), https://doi.org/10.1016/j.matpr.2020.08.094
7. Q. Li, Y. Zhang, Y. Cheng, X. Zuo, Y. Wang, X. Yuan and H. Huang, *Materials (Basel),* **15(4)**, 1621(2022), https://doi.org/10.3390/ma15041621.
8. F. Moro, S. Keβler, and F. Landi, *Proceedings in Civil Engineering*, **6(5)**, 1044(2023), https://doi.org/10.1002/cepa.2044
9. B. Quan, J. Li and C. Chen, *American Chemical Society Omega*, **6(40),** 25904(2021), https://doi.org/10.1021/acsomega.1c02220
10. A. H. Ostovari, S. R. Peikari, S. R. Shadizadeh and S.J. Hashemi*, Corrosion Science*, **51,** 1935(2009), https://doi.org/10.1016/j.corsci.2009.05.024
11. G. Sharma and J. G. Handique, *Asian Journal of Chemistry*, **28(10),** 2223(2016), http://dx.doi.org/10.14233/ajchem.2016.1993
12. P. Burhagohain, G. Sharma, P. M. Bujarbaruah, U. S. Deka, and D. J. Kalita. *Biointerface Research in Applied Chemistry*, **13**, 380(2023), https://doi.org/10.33263/BRIAC134.380
13. P. Burhagohain and G. Sharma*, Letters in Applied NanoBioScience*, **13**, 103(2024), https://doi.org/10.33263/LIANBS133.103
14. O. A. Akinbulumo, O. J. Odejobi and E. L. Odekanle, *Results in Materials*, **5**, 100074(2020), https://doi.org/10.1016/j.rinma.2020.100074
15. S. A. Umoren, U. M. Eduok, M. M. Solomon and A. P. Udoh, *Arabian Journal of Chemistry*, **9(1)**, S209(2016), https://doi.org/10.1016/j.arabjc.2011.03.008
16. R. Kumar, O. S. Yadav and G. Singh, *Journal of Molecular Liquid*, **237**, 413(2017), https://doi.org/10.1016/j.molliq.2017.04.103
17. A. Kokalj, *Corrosion Science*, **217**, 111112(2023), https://doi.org/10.1016/j.corsci.2023.111112
18. S. Chaudhary and R. K. Tak, *Biointerface Research in Applied Chemistry*, **12(2)**, Article 2603(2022), https://doi.org/10.33263/BRIAC122.26032617
19. A. Chaouiki, M. Chafiq, Y. G. Ko, A. H. Al-Moubaraki, F. Z. Thari, R. Salghi, K. Karrouchi, K. Bougrin, I. H. Ali and H. Lgaz, *Metals*, **12(10)**, 1598(2022), https://doi.org/10.3390/met12101598
20. L. Emembolu and P. K. Igbokwe, *Journal of Basic and Applied Research International*. **26(1)**, 23(2020),
21. E. A. Noor, *International Journal of Electrochemical Science*, **2**, 996(2007), https://doi.org/10.1016/S1452-3981(23)17129-X
22. A. Taheri and H. Ahmadi, *Indian Journal of Chemical Technology*, **30**, 67(2023), https://doi.org/10.56042/ijct.v30i1.62034
23. M. Lebrini, F. Robert and C. Roos, *International Journal of Corrosion,* 139798(2013), https://doi.org/10.1155/2013/139798
24. I. Mohammadi, T. Shahrabi, M. Mahdavian and M. Izadi, *Journal of the Electrochemical Society,* **167**, 131506(2020), https://doi.org/10.1149/1945-7111/abb70e

[RJC-9246/2025]